Applications of Computational Mechanics in Geotechnical Engineering, Fernandes et al. (Eds.)
© 2001 Swets & Zeitlinger, Lisse, ISBN 90 5809 114 7

Three-dimensional analyses of the Paraíso tunnel, Brazil

J.Almeida e Sousa
Department of Civil Engineering, University of Coimbra, Portugal
A.Silva Cardoso & M.Matos Fernandes
Department of Civil Engineering, University of Porto, Portugal

ABSTRACT This paper presents the field observations and the results of the application of finite elements models to the construction of the Paraíso tunnel of the S. Paulo metro system. This shallow tunnel, excavated in clayey formations exhibiting a wide range of strength and deformability, has been well-documented by Brazilian authors in a number of studies. The calculations involved three-dimensional analyses with a careful simulation of the entire construction sequence. The mechanical behaviour of the soil was reproduced by using two distinct constitutive laws: the simple elastic perfectly plastic model and the elasto-plastic model developed by Lade (1977, 1979). The observed behaviour is compared with the numerical results. Some conclusions are extracted concerning the limitations and capabilities of the constitutive soil models employed.

1 INTRODUCTION

The successful application of the finite element method to the numerical modelling of the construction of tunnels in soils depends on two factors. The first concerns the simulation of the construction process, particularly the sequence of the excavation and its articulation with the placement of the support. The second factor concerns the constitutive law employed to simulate soil behaviour.

With respect to the first factor mentioned above, it should be noted that, whatever method of tunnelling and supporting is used, a three-dimensional equilibrium is generated in the vicinity of the tunnel heading. Therefore, the actual definition of the stresses and displacements in the surrounding ground and on the support requires that three-dimensional analyses are used.

Regarding the second factor, the constitutive law should reproduce the main characteristics of soil behaviour, namely: i) the stress-strain non-linearity; ii) the occurrence of plastic strains; iii) the influence of the intermediate principal stress; iv) the dilatancy; v) the stress path dependency. A constitutive elasto-plastic model able to reproduce the features mentioned above was proposed by Lade and Duncan (1975), and subsequently developed by Lade (1977, 1979). Though based on results of triaxial tests with the principal stresses varying independently, the model can be calibrated from conventional triaxial and isotropic compression tests.

This paper describes a study on the numerical simulation of the construction of a stretch of the Paraíso metro tunnel in S. Paulo, Brazil, excavated in clayey ground. The calculations involved three-dimensional finite element analyses, with the objective of reproducing the entire construction sequence as close as possible. The Lade's elasto-plastic model and a simpler elastic perfectly plastic model were used for the simulation of soil behaviour. The results provided by on site instrumentation were compared with the values obtained from the calculations.

2 DESCRIPTION OF THE SITE AND OF THE TUNNEL CONSTRUCTION

The tunnel cross-section, shown in Figure 1, has a height of 8.4 m and a maximum width of 11.4 m, corresponding to an area of 82 m^2. The soil cover is approximately 7.6 m.

As Figure 1 also shows, the site investigation revealed the existence of a thin layer of superficial fill, covering two clayey strata (the red clay and the so-called variegated clay) and a layer of very dense clayey sand (Parreira, 1991).

The first of these clayey formations is highly porous (void ratio larger than 1.5) and may be subdivided in two horizons, with the upper one showing more intense weathering (SPT values ranging from 4 to 6 and from 7 to 11, in the upper and lower zones, respectively). The second clay formation, located below the red clay, is a heavily overconsolidated stiff and fissured sandy clay, whose SPT values

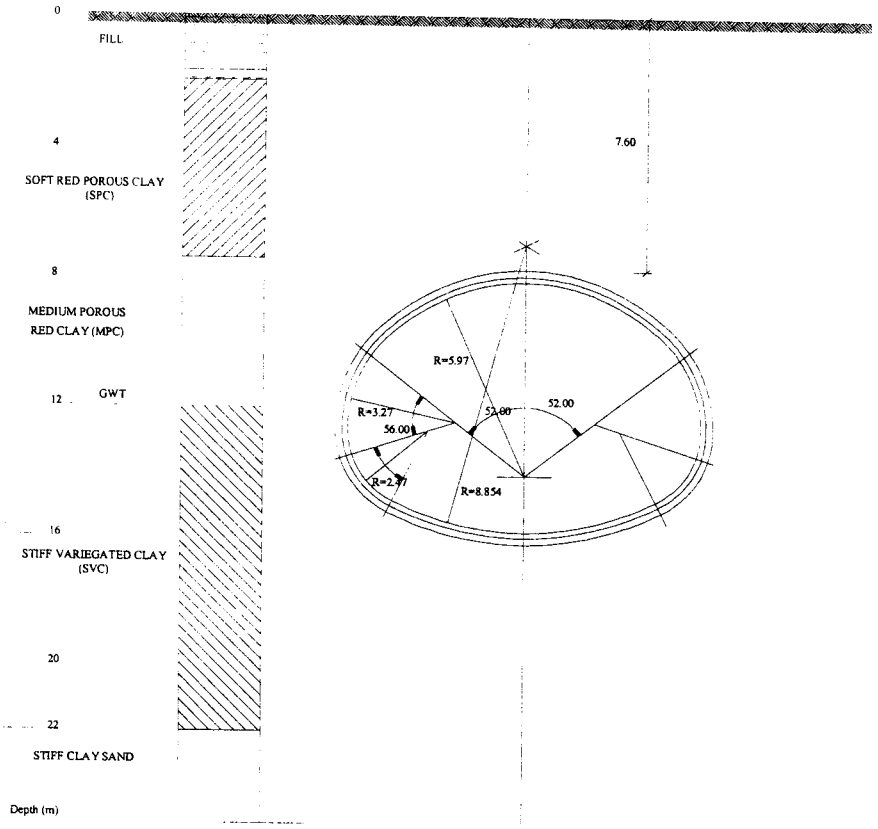

Figure 1 – Paraíso tunnel cross-section and geotechnical profile of the site

range from 16 to 22. The ground-water level coincides with the frontier between the red clay and the variegated clay.

The construction process was based on NATM principles, with the sequence of excavation and placing of primary support following the scheme given in Figure 2.

A stepped profile of crown and bench was adopted. The heading face was advanced in 1.6 m stages leaving a central supporting ground core that was excavated after the crown support installation (steel lattice girders in combination with sprayed concrete 20 cm thick). The bench was excavated in 1.6 m steps, between 3.0 and 4.8 m after the heading face.

Sprayed concrete was applied to a steel mesh immediately afterwards, thus completing the lower part of the arch.

3 FIELD MONITORING

In order to control the construction process and the safety of structures and services in the vicinity, field instrumentation was installed at several locations. Figure 3 shows the location of the observation devices in the section that has been considered for the numerical analyses.

The instrumentation used in the ground adjacent to the tunnel consisted of a number of surface marks to settlement measurements by surveying techniques, 2 multipoint vertical extensometers and one vertical inclinometer. Inside the excavation levelling pins and horizontal bases were installed to measure convergence. It was thus possible to define the profiles of surface settlements, vertical and horizontal displacements in the ground at different depths and

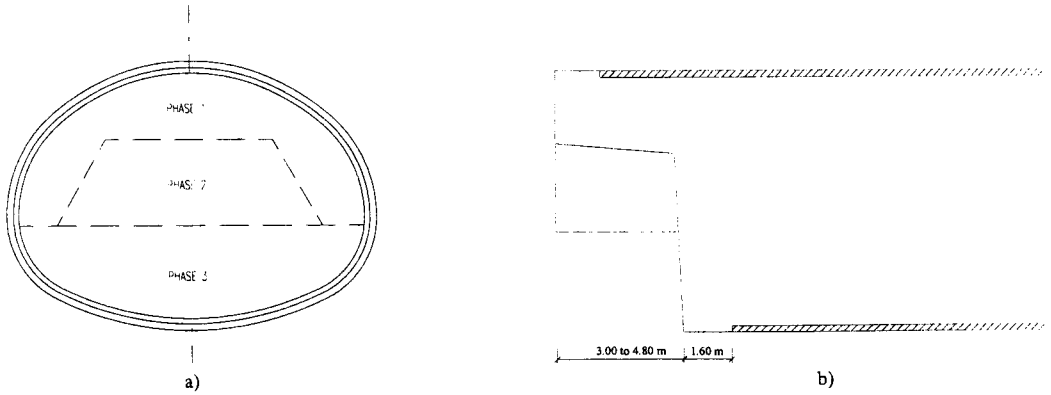

Figure 2 – Construction process used: a) transverse section; b) longitudinal section

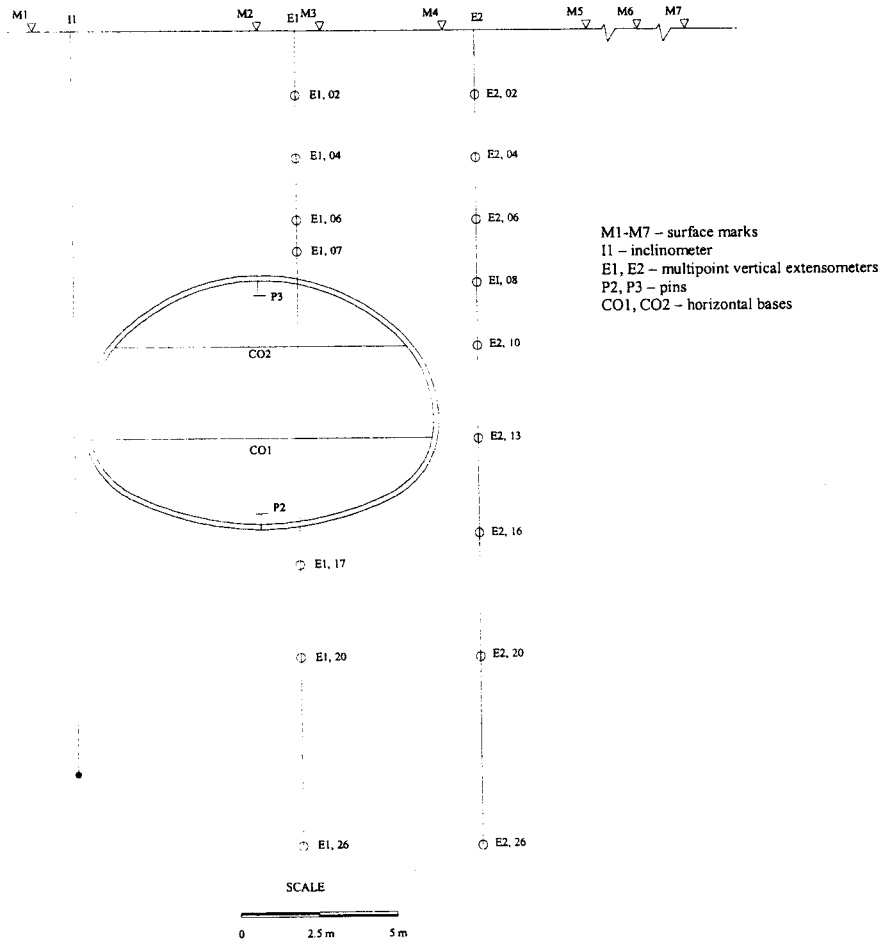

Figure 3 – Location of observation devices

vertical displacements at the roof and invert of the tunnel as well as convergences inside the cavity.

Two of the results given by the site instrumentation deserve a special mention: the transverse profile of the surface settlements and the vertical displacements at points above the crown of the tunnel.

Figure 4 shows the surface settlements profiles corresponding to three measuring phases: one carried out before the monitored section was excavated; another when the tunnel heading reached it, and a third done about 40 days afterwards, when the settlements had virtually stabilised. The same figure presents also the gaussian curve and the yield density curve (Celestino and Ruiz, 1998) that best fit the final settlement profile.

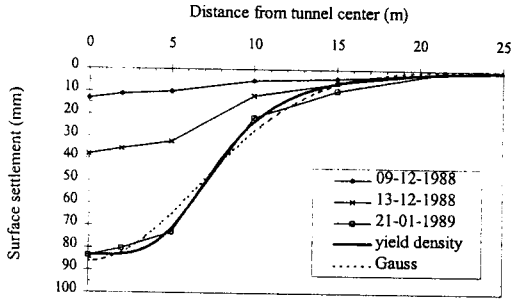

Figure 4 – Surface settlements profiles

The figure reveals certain interesting points:

i the profile of the surface settlements ahead of the tunnel face is relatively level;

ii with the progress of the excavation past the instrumented section the vertical downward movements are mainly limited to the bulk of soil situated above the crown of the tunnel;

iii the final profile of the surface settlements is much better fitted by the yield density curve than by the gaussian.

Figure 5 concerns the angular distortions at the surface, calculated on the basis of the two approximations of the transverse profile of the final settlements mentioned above. It can be seen that the distortions deduced from the gaussian curve are considerably smaller, leading to unsafe predictions of damage on adjacent buildings and services.

Figure 6 depicts the curves representing the vertical displacements of points situated on a vertical axis above the cavity (about 1 m from the centre line). The results of the three measuring phases are also included: the first carried out prior to the excavation

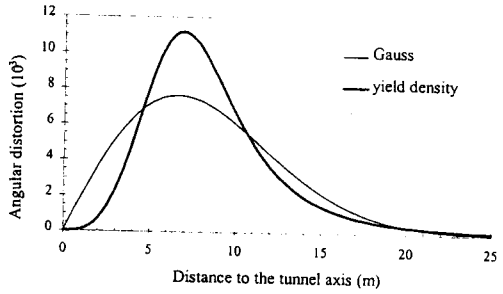

Figure 5 – Angular distortion deduced from the curves used to approximate the transverse profile of the final settlements: gaussian and yield density curves

of the monitoring section, the second taking place when the tunnel heading reached it, and the last performed when the tunnel heading was already far enough away for the deformations associated with the excavation to be considered negligible.

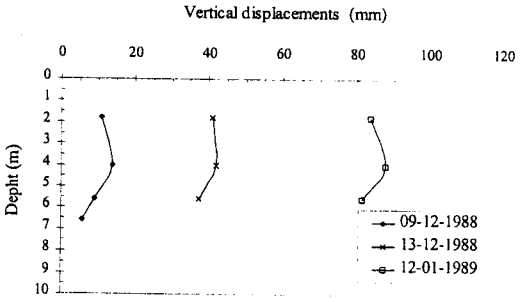

Figure 6 – Vertical displacements of points situated on a vertical axis about 1 m from the centre line

The first aspect highlighted by this figure relates to the fact that, ahead of the tunnel face, the displacements of the points nearest the surface grow more rapidly than at the points near the cavity. This is natural, assuming the existence of a compression zone, caused by the arching effect that develops on the vertical longitudinal section, responsible for transferring the load from the region already excavated, but not yet supported, to the non-excavated region ahead of the tunnel and to the support placed behind (Almeida e Sousa, 1998).

The second aspect is related to the fact that, with the passage of the tunnel heading and its subsequent progression, the soil mass above the cavity undergoes a movement practically as a rigid body, with no reduction of the displacements being observed as the

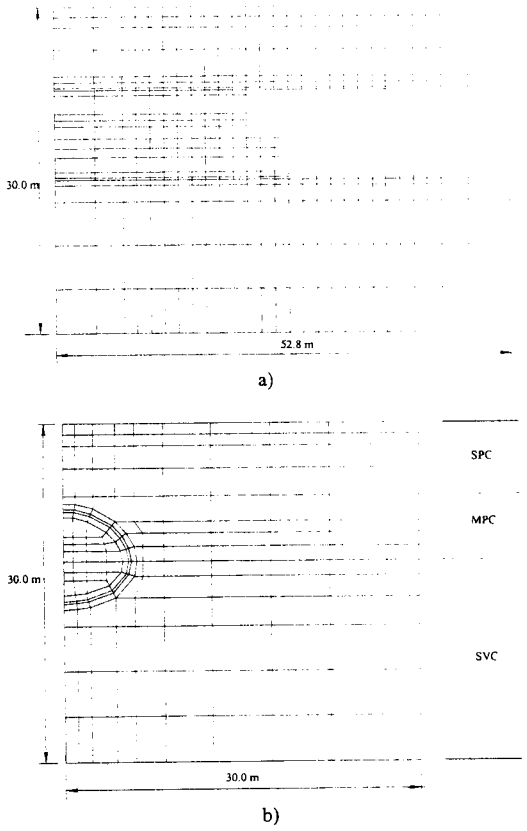

Figure 7 – Finite element mesh adopted: a) longitudinal section; b) transverse section

distance from the cavity increases. According to Ortigão et al. (1996), this is probably due to the collapsible nature of the porous red clay, which might consequently experience a considerable reduction in volume as the tunnel heading advances.

4 FINITE ELEMENT ANALYSES

The numerical studies were performed using a finite element code (Almeida e Sousa, 1998) developed for 2D or 3D structural analysis of geotechnical works, including the construction of tunnels. The code permits the use of several kinds of finite elements, capable of representing the ground, the structural components of the support and the interfaces between the different materials. With respect to modelling the mechanical behaviour of the various materials and their interfaces, a wide menu of constitutive models of variable complexity is available.

The finite elements mesh, on the basis of which the three-dimensional equilibrium was analysed, is reproduced in Figure 7, together with the ground profile considered.

The mesh comprises 5544 nodal points and 5239 elements, among which 5032 are isoparametric elements with eight nodal points, with the remaining 237 two-node bar elements simulating the 12 m wide paved public road, under which the tunnel is being excavated. This representation of the pavement by bar elements is justified by the fact that the thickness of the paving is small in relation to its stiffness (Parreira, 1991).

Longitudinal displacement is restrained at its end sections. In the transverse section, the left lateral boundary, where horizontal displacements at the tunnel axis are prevented, corresponds to the plane of symmetry, and the right lateral boundary has been placed at a distance of 30 m from it, after which such horizontal displacements are held to be negligible. The lower boundary, where displacements were impeded, was placed at a depth of 30 m.

It should be noted that the mesh described above was designed to have the maximum refinement compatible with the capacity of the computer available for this study. It was, indeed, because of this limited capacity that higher order finite elements were not used.

As Figure 7 shows, the construction process was simulated incrementally in the analyses, with the crown and the bench advancing simultaneously. The bench was 4.8 m behind the crown, in terms of excavation progress, and the support structure was closed 6.4 m from the face.

Table 1 includes the values of the unit weight and of the coefficient of earth pressure at rest adopted for the distinct formations into which the ground interested in the tunnel construction was divided.

Table 1 – Parameters defining at-rest state of stress

	γ (kN/m^3)	K_0
SPC	14.7	0.38
MPC	15.0	0.38
SVC	17.9	0.84

Table 2 contains the parameters of Lade's model and the respective values. In order to the account of overconsolitation, it was assumed, according to Zorneberg (1989) that the soil elements exhibit elastic behaviour with respect to volumetric and shear deformations until they reach strain constant values to which the contractive (f_c) and expansive (f_p) yield functions correspond (see Table 3).

It should be noticed that Lade's model was not used for the variegated clay, since parameters of the

Table 2 – Lade's model parameters (Parreira, 1991)

		Soft Red Porous Clay	Medium Porous Red Clay
Elastic	k	98.50	153.97
	n	-0.15	0.57
	ν	0.27	0.27
Collapsive Work-Hardening	p	0.0387	0.0199
Failure Envelope	η_1	138.40	133.63
	m	1.24	0.88
Expansive Plastic Potential	s_1	0.30	0.41
	s_2	0.19	0.00
	t_1	31.39	3.68
	t_2	-58.72	-17.47
Expansive Work-Hardening	P	0.40	0.414
	L	0.37	0.446
	α	0.90	1.65
	β	0.00	0.00

Table 3 – Initial stress levels (Parreira, 1991)

	$(f_c)_0$ (kPa)^2	$(f_p)_0$
SPC	27208	8.64
MPC	63600	10.48
SVC	1305544	5.35

Table 4 – Parameters of the elastic perfectly plastic model (Parreira, 1991)

	E′ (MPa)	ν′	c′ (kPa)	ϕ′ (°)
SPC	4	0.27	35.4	23.3
MPC	6	0.27	39.8	27.2
SVC	120	0.17	66.2	25.0

model obtained by Parreira did not include the cohesive component of shear strength; the absence of this component lead to numerical instability in the elements representing the bench. To overcome this, the elastic perfectly plastic model was used for the variegated clay stratum. Table 4 shows the values of the parameters for this last model, for all the soils. For the Young's modulus secant values corresponding to 50% of the failure shear stress were used. It was found that the soils did not exhibit positive dilatancy, therefore a law of non-associated plastic potential defined by the Von Mises surface was employed, such that the volumetric component of the plastic deformation was null.

With regard to the components of the structural support, an elastic, linear and isotropic behaviour was assumed, characterised by the following values of Young's modulus and Poisson's coefficient: $E = 10$ *GPa* and $\nu = 0{,}2$. Furthermore, concerning the support's stiffness, it should be noted that the initial modulus of elasticity of the sprayed concrete (arch not yet closed at the invert) was defined so that the calculated final settlement at the surface above the axis of the tunnel would be equal to the observed values. In both analyses the value thus defined was approximately 0.6 *GPa*.

Finally, the pavement, mentioned earlier, was simulated by means of bar elements with a thickness of 40 cm and linear elastic behaviour, with a Young's modulus $E = 1$ *GPa*.

5 CALCULATION RESULTS

Figure 8 illustrates the evolution over distance from the tunnel heading of the vertical displacements of points of the surface and of the crown belonging to the tunnel plan of symmetry, calculated with the Lade's model.

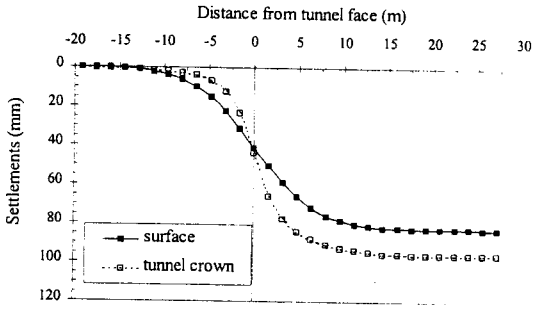

Figure 8 – Evolution with the advance of the tunnel of the vertical displacements of surface and crown points on the plan of symmetry - results obtained with Lade's model

The difference between the values represented by the curves of Figure 8, which represents the relative vertical displacement of the surface and the crown, can be observed in Figure 9, together with the vertical (radial) stresses in the crown. The evolution of the relative vertical displacement reflects particularly well the one of the vertical stresses. Ahead of the tunnel face, where the longitudinal arching causes an increase of vertical stress, the displacement of the crown is smaller than that of the surface. With the passage of the excavation face, the vertical stress sharply drops, tending to evanesce in the non-supported zone. A much stronger variation rate of the crown displacement is consequently observed, reaching its highest value relative to the surface. Following the installation of the tunnel lining, the vertical stress experience a new increase, with the

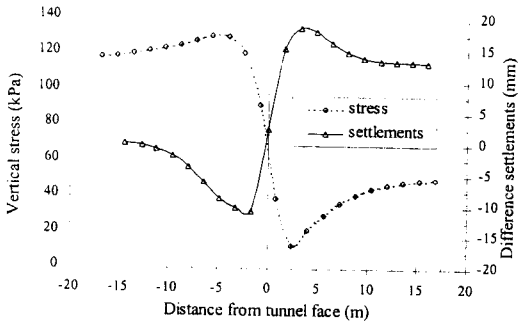

Figure 9 – Evolution with the tunnel advance of the relative vertical displacement of the surface and the crown and of the radial stress in the crown - results obtained with Lade's model

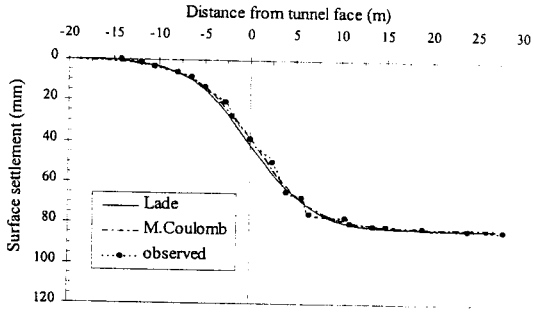

Figure 10 – Longitudinal profile of surface settlements – comparison of observed results with the calculated using Lade's and the elastic perfectly plastic models

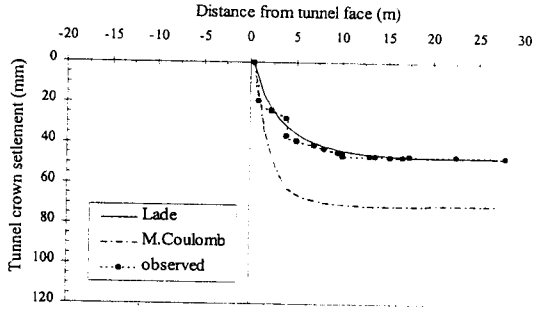

Figure 11 – Evolution of vertical displacement of the tunnel roof with the progress of the excavation – comparison of observed results with those given by Lade's and the elastic perfectly plastic models

relative displacement decreasing, to produce a final value of approximately 13 mm.

Figure 10 shows the evolution, as the tunnel heading advances, of the observed maximum surface settlements and their comparison with the values obtained

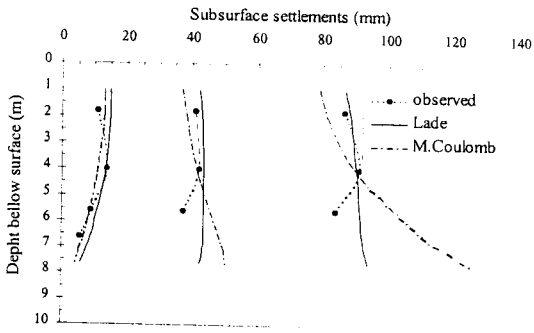

Figure 12 – Evolution with depth of the vertical displacements above of the tunnel – comparison between the observed results and those given by the elastic perfectly plastic and Lade's models

from the finite element analyses with the two constitutive models mentioned above. Figure 11 shows the comparison of the evolution, after the excavation of the section, of the calculated vertical displacement of the tunnel roof with the observed at a pin installed there.

The first conclusion to be drawn from Figures 10 and 11 is that there is good agreement between the measured displacements and those calculated using the model developed by Lade. In fact, not only does the final calculated surface displacement value coincide with the observed – a condition imposed by the definition of the initial stiffness of the sprayed concrete – but its evolution derived from the calculation and the roof displacement are significantly close to the measured values.

It can further be seen from Figure 10 that the elastic perfectly plastic model properly reproduces the evolution of the maximum vertical displacement of the surface. The same does not apply, however, to the evolution of the vertical roof displacement. In fact, as can be seen from Figure 11, the calculated displacement using the elastic perfectly plastic model is significantly greater than the observed value.

Apart from the zone in front of the tunnel heading, the vertical measured and calculated displacements above the cavity are clearly discrepant, as expressed by Figure 12. In fact, the observed displacements decrease with depth with the approach and passage of the tunnel heading while the numerical results reveal an increase with depth – which is very slight in the case of the Lade's model and very pronounced for the elastic perfectly plastic model.

The considerable increase of vertical displacements above the tunnel, once the section had been excavated, obtained with the elastic perfectly plastic model, may be explained by the inability of the

model to reproduce the dependency of the mechanical behaviour of the soil on the stress path. Indeed, the fact that, after excavation of the section, a vast zone of elements above the cavity experience unloading – a decrease in shear stresses – confers a higher stiffness to the soil situated there. Obviously, this cannot be taken into account by a model whose elastic parameters were obtained from the primary loading stress-strain curves from conventional triaxial tests.

In Figure 13, a comparison is made between the transverse profiles of the surface settlements, calculated with Lade's model, and those provided by the observation for the three stages shown in Figure 4. Besides the reasonable agreement between the maximum values, another feature that should be noted concerns the evolution of the transverse profile as excavation progresses. The calculation shows an important restriction on the vertical displacements above the cavity, which is exactly what was observed.

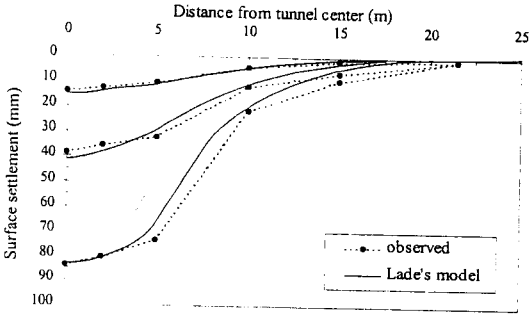

Figure 13 – Evolution of transverse profiles of the surface settlements – comparison of experimental results and those obtained from Lade's model

With regard to the width of the strip on the surface that is influenced by the tunnel, the examination of the above figure reveals that it was slightly underestimated by the numerical analysis. This underestimation could be linked to the very low value taken for the coefficient of earth pressure at rest for the porous red clay (Almeida e Sousa, 1998).

Comparison of the results of the two numerical calculations with respect to the transverse profile of the final surface settlements is given in Figure 14. Despite the good approximation of the values of the maximum settlement and of the width of the surface strip affected by the excavation, the shape of the curves is different. Contrary to what was observed, and to the result of the elasto-plastic Lade model, the curve produced by the elastic perfectly plastic calculation has a shape that is similar to a gaussian curve, thereby giving a significant underestimation

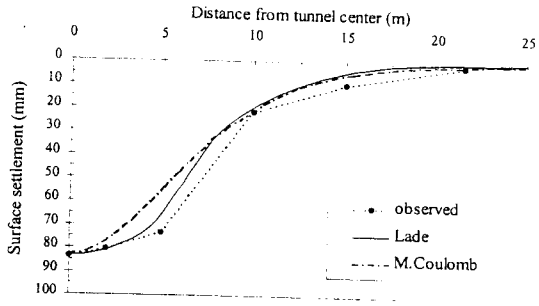

Figure 14 – Transverse profile of the final settlements at the surface – comparison between the results observed and those given by the elastic perfectly plastic and Lade models

of the maximum angular distortion.

Some important differences are also observed in the horizontal displacements perpendicular to the tunnel axis given by the elastic perfectly plastic and the Lade's models, as Figure 15 illustrates. The maximum values obtained with the first model are higher and occur at greater depth.

6 CONCLUSIONS

The main conclusions of the study can be summarised as follows.

As regards the results observed on site, the following should be noted:

i vertical downward movements were mainly concentrated in the block of soil above the tunnel, thus giving rise to a high maximum angular distortion value at the surface; as a result, the respective transverse profile of the settlements was not properly fitted by the gaussian curve;

ii a good approximation of the aforementioned transverse profile was achieved using a yield density curve;

iii there was no attenuation of the vertical movements with increasing distance from the crown of the tunnel; indeed, the displacements recorded near the surface are even a little higher than those obtained close to the opening.

The following findings resulted from the three-dimensional numerical analyses:

i even though lower order three-dimensional finite elements were used, the results of the analyses in which the behaviour of red clay was simulated using Lade's model reproduced the global observed results very reasonably; in particular, the evolution with the progress of the excavation of the trans-

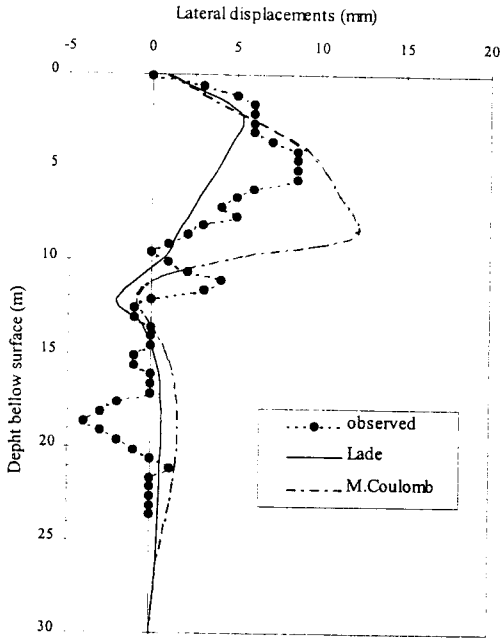

Figure 15 – Displacements perpendicular to the tunnel axis – comparison of the observed results and those given by Lade's and the elastic perfectly plastic models

verse profile of the surface settlements and the vertical displacement of the tunnel roof showed good agreement.

ii the comparison of the analytical results obtained with the two elasto plastic models underlines the remarkable influence associated with the constitutive law employed to represent the mechanical behaviour of the soils involved by the tunnel excavation; despite the similarity of the maximum surface settlements, the values of maximum angular distortion and vertical displacements above the cavity supplied by the two calculations are considerably distinct; the values of the horizontal displacements perpendicular to the tunnel axis also differ, with the elastic perfectly plastic model giving higher maximum values, which occur at greater depth.

ACKNOWLEDGEMENTS

The authors would like to express their gratitude to the project and consulting firm *BUREAU*, in the person of Professor Arsénio Negro Jr., and to the Companhia do Metrô de S. Paulo, in the persons of Sérgio Salvadori and Argimino Ferreira, for furnishing the main results observed on site.

REFERENCES

Almeida e Sousa, J. (1998). Tunnelling in Soils. Geotechnical Behaviour and Numerical Simulation (in Portuguese). *PhD Thesis, University of Coimbra.*

Celestino, T. B.; Ruiz, A. P. T. (1988). Shape of settlement throughs due to tunnelling. Through different types of soft ground. *Felsbau 16, pp. 118-121.*

Lade, P. V.; Duncan, J. M. (1975). Elastoplastic stress-strain theory for cohesionless soil. *Journal of the Geotechnical Engineering Division, ASCE, Vol. 102, GT10, pp. 1037-1053.*

Lade, P. V. (1977). Elasto-plastic stress-strain theory for cohesionless soil with curved yield surfaces. *International Journal of Solids and Structures, Vol. 13, pp. 1019-1035.*

Lade, P. V. (1979). Stress-strain theory for normally consolidated clay. *Proc. 3th Int. Conf. on Numerical in Geomechanics, Aachen, Vol. 4, pp. 1325-1337.*

Ortigão, J. A. R.; Kochen, R.; Farias, M. M.; Assis, A. P. (1996). Tunnelling in Brasília porous clay. *Canadian Geotechnical Journal, Vol. 33, pp. 565-573.*

Parreira, A. B. (1991). Analysis of Shallow Tunnels in Soil. The Mineiro Paraíso Tunnel at Paulista Avenue in S. Paulo City (in Portuguese). *PhD Thesis, PUC, Rio de Janeiro.*

Zornberg, J. G. (1989). Finite Element Analysis of Excavations Behaviour Using an Elasto-Plastic Model (in Portuguese). M.Sc. Thesis, *PUC, Rio de Janeiro.*